An integral process model for high precision composite forming

Remko Akkerman — Edwin A.D. Lamers — Sebastiann Wijskamp

University of Twente
Faculty of Engineering Technology
Composites Group PO Box 217
7500 AE Enschede
the Netherlands

R.Akkerman@ctw.utwente.nl
E.A.D.Lamers@ctw.utwente.nl
S.Wijskamp@ctw.utwente.nl

ABSTRACT. *High precision composite forming implies control of the fibre orientation, residual stresses and wrinkling in the product to be manufactured. Finite Element based process simulations can assist in achieving this right-first-time manufacturing. A first order approximation of the full manufacturing process is presented in a three-step approach: a multilayer Finite Element drape simulation, a micromechanics based stiffness and stress prediction and a Finite Element trimming and spring-back prediction. A wing leading edge stiffener is presented as a validation exercise, based on which the future research topics in Composite Forming are discussed.*

RÉSUMÉ. *La mise en forme à haute précision de composites nécessite de contrôler, lors de la fabrication du produit, l'orientation des fibres, les contraintes résiduelles et le plissement. La simulation de procédés basée sur les éléments finis est utile à la réalisation de cet objectif de fabrication correcte du premier coup. Une approximation au premier ordre du procédé de fabrication est présentée selon une approche en trois phases : une simulation du drapage multicouche, une prédiction de la raideur et des contraintes reposant sur la micromécanique, et une prédiction par éléments finis du retour élastique. Le cas d'un raidisseur primaire d'aile est traité comme exemple de validation, et sert de support à une discussion de perspectives de recherche en mise en forme de composites.*

KEYWORDS: *thermoplastic composites, forming simulations, spring-back.*

MOTS-CLÉS : *composites thermoplastiques, simulation de mise en forme, retour élastique.*

Revue européenne de mécanique numérique. Volume 15 – n° 4/2006, pages 359 to 377

1. Introduction

Woven fabric reinforced composite materials are typically applied in plate or shell structures, such as ribs, stiffeners and skins. Products of these materials can be manufactured with several processes. A few examples of these composite forming processes are compression moulding, diaphragm forming, matched metal die forming and Rubber Press Forming (RPF), which are specifically suited for the rapid forming of fabric reinforced thermoplastics. Shape distortions can occur during manufacturing of composite products. During the development stage of the products these distortions often exceed the dimensional accuracy required in the aeronautical and car industry. The demanded accuracy can be met by adapting the mould shape to account for the shape distortions. This procedure is based on costly trial and error methods. Development costs can be reduced by modelling the shape distortions on beforehand and adapting the mould shape accordingly, aiming for a "right first time" production process.

High precision composite forming implies, in general terms, control of the fibre orientation, residual stresses and wrinkling in the product to be manufactured. Regarding the complexity of the materials and the processes, this can only be achieved with proper and accurate modelling of the material and the process conditions this material is subjected to. Figure 1 schematically summarises the relevant phenomena, with the process conditions, the laminate and tool geometries and the laminate lay-up as the governing input parameters.

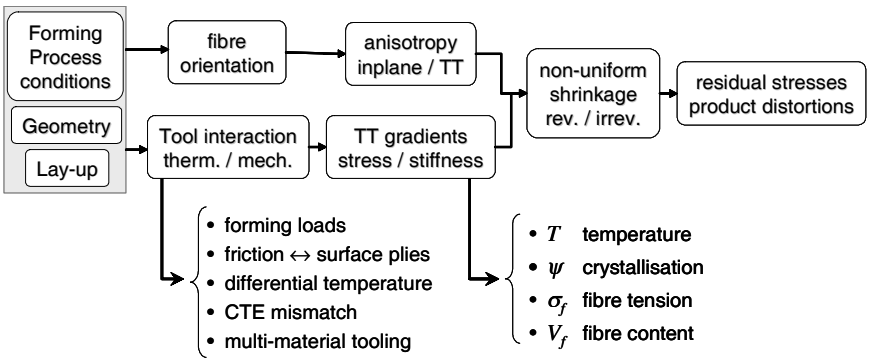

Figure 1. *Functional scheme of the origins of composite shape distortions*

The first terms to take into account in the distortion analysis are the mechanical properties (stiffness) and thermal expansion behaviour (shrinkage and warping), referred to as the thermomechanical properties of the product. The shape distortions can be introduced by, for example, thermal loading or stresses induced by forming. Obviously, the materials used and the lay-up of the composite affect the resulting

properties. However, due to process induced fabric reorientation, the thermomechanical properties of the composite change locally as a function of the fibre reorientation. The fibre orientation distribution and resulting local anisotropic composite properties need to be taken into account in order to model the product distortions. For instance, the difference in inplane and through-thickness ("TT") properties causes the spring-forward phenomenon (Wiersma *et al*., 1998). An inhomogeneous distribution of these properties will lead to non-uniform shrinkage and hence to further product distortions. The simplest approximation would hence follow only the upper branch in Figure 1, from fibre orientation and resulting anisotropy to non-uniform shrinkage and product distortions.

In addition, the interaction of the product with the tools can induce residual stresses. The consolidation pressure will be released when the product is ejected, usually leading to anisotropic expansion. Friction during forming affects the deformation of the laminate as a whole, but the surface plies will be subjected to a different load than the inner plies. The tool temperatures will not be uniform for the rapid pressing processes considered and neither will be the temperature in the laminate. The thermal expansion of tools and laminate will most likely differ, which again leads to loads introduced on the laminate during processing. Using multi-material tooling, such as a steel and a rubber mould half, further complicates the matter.

These effects will typically lead to variations through the thickness of the laminate, in other words through-thickness gradients in temperature, crystallisation (in the case of semi-crystalline matrix material), fibre tension and fibre content. These, in turn, usually cause bending moments, which may lead to considerable warping.

The combination of all loads with the laminate properties leads to a non-uniform distribution of anisotropic shrinkage and residual stresses which cause product distortions once the product is released. More or less artificially, a distinction can be made between reversible and irreversible effects, with thermal expansion as the most prominent reversible effect. Especially these reversible effects can be investigated experimentally, in order to validate various model assumptions. It is well-known, however, that these reversible effects only cause a limited portion of the total shape distortions (Wiersma *et al*., 1998). Many competing factors of the same order of magnitude play a role in high precision composite forming.

Only a few authors modelled the shape distortions of thermoplastic composites including process induced fibre reorientation. (Hsiao *et al*., 1999) modelled the complete thermoforming process of thermoplastic composites. They account for fibre reorientation during forming and the evolution of the microstructure of the fabric weave in the nonisothermal simulation. (Sweeting *et al*., 2002) modelled the deformation of curved circular flanged thermosetting laminates due to thermoforming. Spring-forward was incorporated in the model, while neglecting the effects of the microstructure of the weave. Hofstee coupled a kinematical drape

modeller to a woven fabric analysis on a pyramid-shaped product (Hofstee *et al.*, 2002), thus accounting for the geometrical changes induced by forming.

The industrial process usually consists of heating and draping multi-layered laminates of non-uniform orientation through the thickness, which are cut to net shape after release from the mould. None of the referenced authors have addressed this complete production chain. The objective here is to predict the shape distortions in the net shaped product after composite forming using a Finite Element (FE) method with computationally efficient plate elements. Tool corrections can be made on beforehand with this design tool, if necessary, preventing the costly trial-and-error optimisation. To this end, we specifically consider the rubber forming process, which is split into three steps (Figure 2):

(I) composite forming: pressing the laminated pre-form on the tooling,

(II) cooling: transferring the heat from the hot laminate to the environment,

(III) finishing: taking the product from the tool and cutting it to its net shape.

The first step considers forming of the woven fabric reinforced plastic material, with the resin in a viscous state, on the tool. This draping process induces reorientation of the fibres, which is one of the effects causing shape distortions. Cooling the composite laminate in the second step leads to inhomogeneous shrinkage, this is often accompanied by warpage. The fibre orientation plays an important role in this shrinkage distribution. The product geometry is changed in the third step by e.g. cutting the product to net shape. This can lead to further shape distortions ("spring-back") by releasing residual stresses.

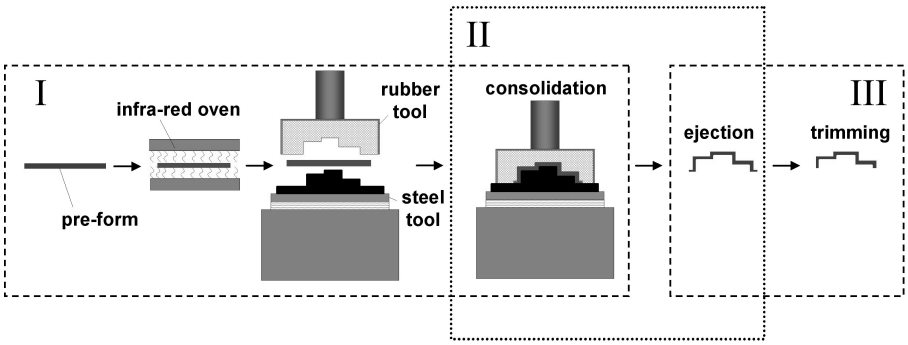

Figure 2. *Schematic overview of the composite forming process using steel and rubber tooling*

2. Process simulation

The three simulation steps will be discussed in more detail: the finite element drape simulation, the micromechanics based residual stress prediction and the non-linear trimming and spring-back simulation.

2.1. *FE Drape simulation*

The draping process was simulated using an implicit FE approach, applying simple triangular membrane elements with wrinkling stabilisation (Vreede, 1992) in the FE package DiekA, which is developed at the University of Twente. The specific composite material behaviour was described using an extended version of the Fibre Reinforced Fluid model (Spencer, 2000). Spencer derived an expression for the linear incompressible anisotropic viscous response of the resin material with inextensible fibres. The Cauchy stress tensor σ can be expressed in terms of the dyadic products of the fibre directions a and b, indicated with the tensors ***A, B, C*** and the rate of deformation ***D***. The extended version of this constitutive model (Lamers *et al*., 2002) allows for compressibility of the resin, extensibility of the fibres, which are attributed a stiffness E, and a contribution of shear locking. This can be summarised as:

$$\begin{aligned}\boldsymbol{\sigma} = &-p\boldsymbol{I} + V_{fa}E_a(\lambda_a - 1)\boldsymbol{A}^* + V_{fb}E_b(\lambda_b - 1)\boldsymbol{B}^* + \\ &+ \frac{1}{2}(V_{fa} + V_{fb})m(\mathrm{e}^{n\theta} - \mathrm{e}^{-n\theta})(\boldsymbol{C}^* + \boldsymbol{C}^{*T}) + \\ &+ V_m[2\eta\boldsymbol{D}^* + 2\eta_1(\boldsymbol{A}^*\cdot\boldsymbol{D}^* + \boldsymbol{D}^*\cdot\boldsymbol{A}^*) + 2\eta_2(\boldsymbol{B}^*\cdot\boldsymbol{D}^* + \boldsymbol{D}^*\cdot\boldsymbol{B}^*) + \\ &+ 2\eta_3(\boldsymbol{C}^*\cdot\boldsymbol{D}^* + \boldsymbol{D}^*\cdot\boldsymbol{C}^{*T}) + 2\eta_4(\boldsymbol{C}^{*T}\cdot\boldsymbol{D}^* + \boldsymbol{D}^*\cdot\boldsymbol{C}^*)]\end{aligned}, \qquad [1]$$

in which p is the hydrostatic pressure, V is the volume fraction of the constituents, λ the stretch of the fibres, n, m and θ describe the shear locking behaviour and η a viscosity. The asterisks indicate a transformation of the tensors to conform to Spencer's original description of a Fibre Reinforced Fluid.

Subsequently, a multi-layer drape material model was developed and implemented, using the same membrane elements (Lamers e*t al*., 2003, 2004). A resin rich layer is assumed between the subsequent fabric layers, causing a viscous friction formulated as:

$$\boldsymbol{\tau} = \frac{1}{\beta}\boldsymbol{v}_{rel}, \qquad [2]$$

with traction τ, slip coefficient β and $\boldsymbol{v}_{rel}$ as the velocity difference between the layers. It was decided not to solve the individual layer deformations in the global FE

system. Instead, a split approach was implemented, in which only the average laminate displacement increments (Figure 3) are solved on the global level.

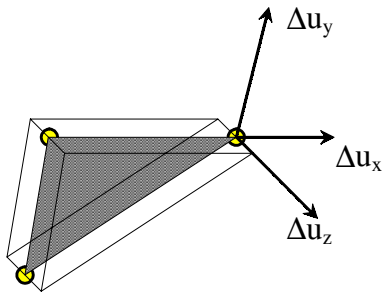

Figure 3. *Triangular element with three displacement degrees of freedom per node*

On the local level (within the element, Figure 4), the velocities and strain rates of the individual layers are solved, assuming a linear velocity field in each layer i,

$$\begin{aligned} v_x^i &= a_1^i + a_2^i x + a_3^i y \\ v_y^i &= b_1^i + b_2^i x + b_3^i y \end{aligned}, \qquad [3]$$

with constants a_j^i and b_j^i.

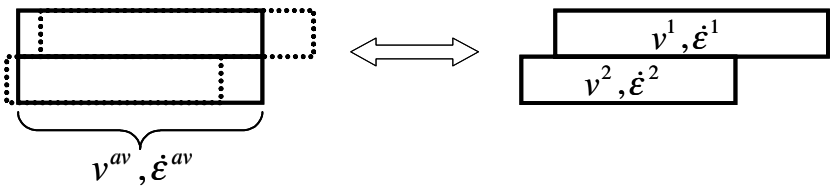

Figure 4. *Two-dimensional representation of the averaged global deformations and the local deformations of two layers within one layered element*

Given the averaged displacements and strains, the individual layer deformations can be found by minimising the total power in the element, subject to the external loads on each layer from the adjacent elements,

$$P = \sum_{i=1}^{nlay} P_{ly}^i + \sum_{j=1}^{nlay-1} P_{int}^j + \sum_{i=1}^{nlay} \sum_{k=1}^{nside} P_{tr}^{ki}, \qquad [4]$$

where the contributions of the layers, the interfaces and the edges with the adjacent elements are specified as:

$$P_{ly}^{i} = \int_{\Omega_{ly}^{i}} \boldsymbol{\sigma}^{i} : \boldsymbol{D}^{i} \, d\Omega_{ly}^{i} \,,$$

$$P_{int}^{j} = \int_{\Phi_{ly}^{i}} \frac{1}{\beta^{j}} \boldsymbol{v}_{rel}^{\ j} \cdot \boldsymbol{v}_{rel}^{\ j} \, d\Phi_{int}^{j} \,, \qquad [5a, b, c]$$

$$P_{tr}^{ki} = \int_{\Gamma_{tr}^{ki}} \boldsymbol{t}^{ki} \cdot \boldsymbol{v}^{ki} \, d\Gamma_{tr}^{ki} \,.$$

The total power P is minimised while the average velocities and displacements are constrained to the global laminate values. The layer parameters a_j^i and b_j^i are found by solving the corresponding system of equations.

After each time step, the properties of the displaced layers are remapped on the new average element geometry, using a convection scheme as described in (van Haaren *et al*., 2000). This Arbitrary Lagrangian Eulerian (ALE) method was implemented in a split scheme, solving the convection problem with an explicit method outside the Newton-Raphson equilibrium iterations. This leads to a small unbalance (provided the convective displacements are small), which is corrected in the equilibrium iterations of the following time step.

The multi-layer drape behaviour thus requires only one element through the laminate thickness. As a result, the number of Degrees Of Freedom (DOF) remains the same for single- and multi-layer drape simulations, albeit at the cost of more effort on the element level. Solving of the FE matrix-vector system is, however, comparable for single and multi-layer simulations.

Multi-layer simulations were presented in (Lamers *et al*., 2003) on the academic Double Dome geometry. In these simulations the friction of the laminate with the tool was assumed similar to the interlayer friction, using the same viscous description. Inertia terms were added to the implicit FE system, resulting in rapid convergence of the iterative solvers (Meinders *et al*., 2003). Simulation times for draping quasi-isotropic laminates were in the order of 60 minutes on a medium class PC.

It was shown that the drape behaviour of multi-layered woven fabric composites depends strongly on the lay-up of the laminate. The drape model results were compared with experiments and confirm the clear dependency between the drape behaviour and the laminate lay-up. The model provides a computationally attractive tool to model draping of multi-layered composites.

2.2. *Micromechanics and residual stresses*

The drape simulation results are used as the input for the stiffness and residual stress predictions. To this end, a generic geometry description of the fabric is assumed, with a variable fibre orientation (Lamers *et al*., 2000). A unit cell, or Representative Volume Element (RVE), can be identified in any regular woven fabric. Figure 5 illustrates this unit cell for Ten Cate's SS303 8-Harness satin weave. Four basic elements can be distinguished within these unit cells (Figure 6), in which each of the yarns can be either straight or undulated. An elliptical cross section, possibly with a straight mid-section, was found to be an appropriate idealised representation of the actual bundle geometries. The centreline of the bundles is compatible with the cross section of the transverse bundles: partially undulated where the bundles are in contact and straight where the bundles are not in contact. Any biaxial weave can be modelled with these basic elements. A volume of resin can be present in between the yarns and on an outer layer, depending on the geometric parameters chosen. These geometric parameters are based on cross-sectional views of the composite laminate.

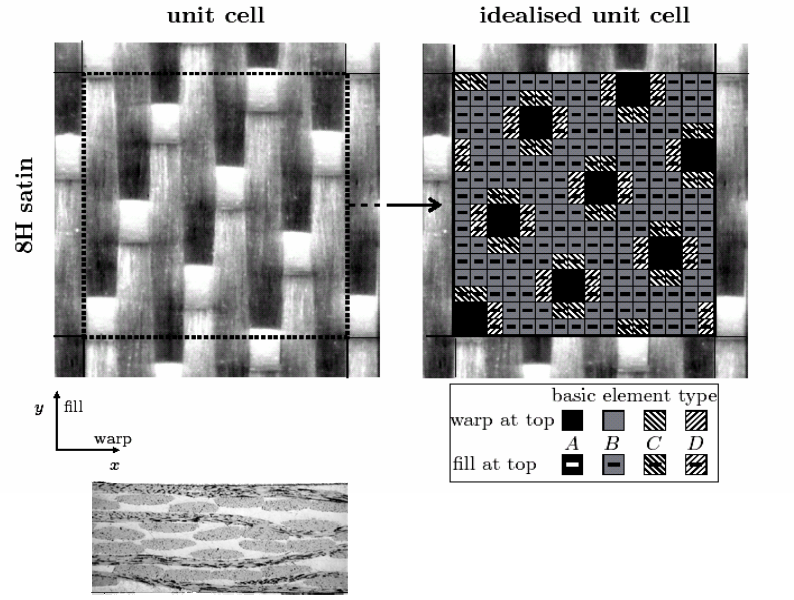

Figure 5. *Top view and cross-section (bottom) of the micro-geometry of an 8H satin glass weave*

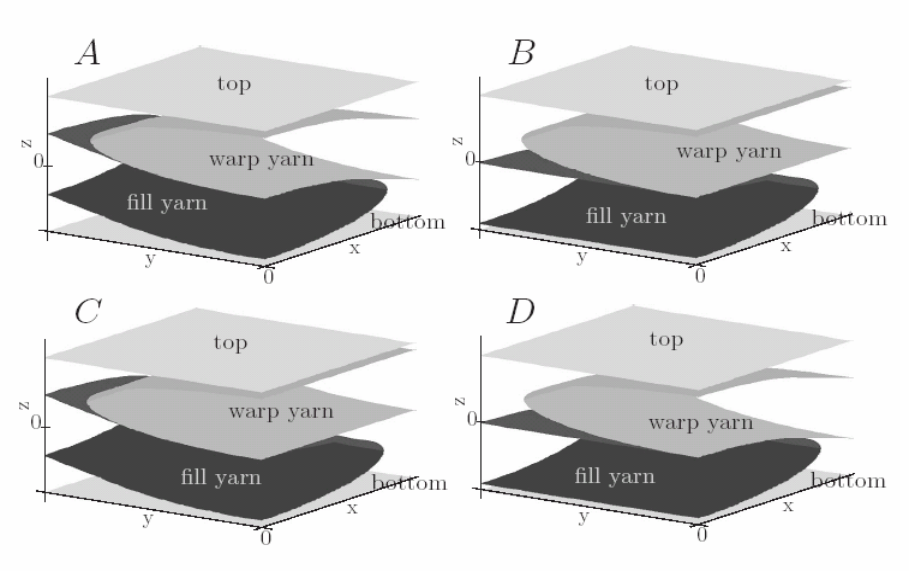

Figure 6. *Basic elements in biaxial woven fabric reinforced composites*

A simple geometric transformation is used when the cell is skewed,

$$\begin{Bmatrix} x' \\ y' \end{Bmatrix} = \begin{bmatrix} 1 & 0 \\ \cos\varphi & \sin\varphi \end{bmatrix} \cdot \begin{Bmatrix} x \\ y \end{Bmatrix}, \qquad [6]$$

with x and y as the original orthogonal axes, as illustrated in Figure 7.

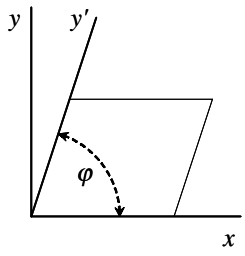

Figure 7. *Shear transformation due to fibre reorientation*

The volume can be assumed constant during shear deformation, which implies that the thickness increases according to:

$$h'(x', y') = \frac{h(x, y)}{\cos(\varphi_0 - \varphi)}, \qquad [7]$$

where $h(x,y)$is the thickness of the ply corresponding to the initial fabric angle φ_0.

A uniform fibre content is assumed for the laminate on the macroscopic scale. The assumed micro-geometry then dictates the local fibre content within the impregnated yarns. The yarn properties are predicted using micro-mechanics, in this case the Composite Cylinder Assemblage (Hashin, 1983) in combination with Schapery's model for the coefficients of thermal expansion. A CLT (Classical Laminate Theory) based method is then applied to determine the local laminate stiffness (ABD-matrix) and thermally induced forces N^{th} and moments M^{th},

$$\left(\overline{A}_{ij}, \overline{B}_{ij}, \overline{D}_{ij}\right) = \frac{1}{S}\int_S\int_h Q_{ij}\cdot\left(1, z, z^2\right) dz\, dS\,,$$
$$\left(\overline{N}_i^{th}, \overline{M}_i^{th}\right) = \frac{1}{S}\int_S\int_h Q_{ij}\alpha_j \Delta T\cdot\left(1, z\right) dz\, dS\,, \qquad [8a, b]$$

with S and h as the surface and the thickness of the basic cell respectively, Q as the stiffness matrix, α as the coefficient of thermal expansion and ΔT as the temperature increment. The local fibre orientations from the drape simulation determine the actual skewed geometry (S and h) of the cell.

These local properties are subsequently averaged to determine the thermo-mechanical properties of the RVE of a single layer and, subsequently, of the laminate as a whole. The thermally induced forces and moments of the laminates are based on the properties at room temperature, assuming temperature independent properties of matrix and fibres. The model was validated on skewed 5H satin carbon fibre reinforced poly(phenylenesulphide) (PPS) laminates (Lamers *et al*., 2000) and on 8H satin glass fibre reinforded PPS (Lamers, 2004). This iso-strain approach was shown to be fairly accurate when compared to a local finite element model as well as to the experiments.

The drape simulation predicts the fibre orientations and the fibre stresses per layer in each element. This information is stored for all integration points of the elements, together with the other state variables. All state variables are updated incrementally during the simulation and stored for the next step. Normally, when stopping the FE simulation, the nodal information is stored for post processing purposes. Here, additional to the nodal information, the element information is stored in a file. The simulation is restarted by reading the element and nodal data from this file. Manipulating this restart-file can effectively change the type of

simulation. The thermo-mechanical module computes the CLT based solution, including thermal and mechanical loads, per element integration point taking into account the fibre reorientation. The state variables from the drape simulation are then replaced by the state variables required for a CLT based simulation. The CLT based simulation uses Discrete Kirchhoff Theory (DKT) triangular elements in order to account for bending. The mesh resulting from draping is used as a reference mesh for the cooling simulation. A second simulation is then started with the "new" state variables and DKT elements, in order to predict the shape distortions during cooling.

2.3. *Trimming and spring back*

One intermediate step has to be taken before the shape distortions can be predicted in the final product, however. Cutting of the excess edges will affect the component stiffness as well as the process induced loads in the component. Moreover, the folds and wrinkles in the areas which are to be removed lead to convergence problems in the geometrically nonlinear spring-back simulation in which the tools are removed and the product is left free to deform due to the process induced residual stresses.

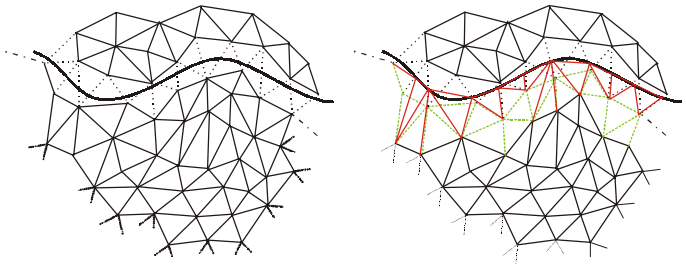

a) b)

Figure 8. *Finite element trimming procedure. a) the trim line cuts through the dotted elements in order to remove the upper part; b) the region near the trim line is remeshed and nodes are centred if necessary*

To this end, the finite element trimming procedure as described in (Avetisyan, 2003) is employed. The excess region is separated by a trim line from the final product geometry. This trim line will generally not coincide with the element edges but will cut through the elements instead. The nodes of these elements will be repositioned in order to conform to the trim line. A local remesh will be applied, including a centring procedure if necessary to improve the shape and size of the elements (see Figure 8). This minimises the mesh disturbance and the resulting inaccuracies in the spring-back prediction. The element data (stresses, fibre orientations, etc.) are remapped on the new finite element mesh. The excess elements are simply removed from the simulation.

The process induced forces and moments are introduced as internal loads in the right hand side of the Finite Element system after trimming, symbolically represented as:

$$\int_S \begin{bmatrix} B_m & 0 \\ 0 & B_b \end{bmatrix}^T \cdot \begin{bmatrix} A & B \\ B & D \end{bmatrix} \cdot \begin{bmatrix} B_m & 0 \\ 0 & B_b \end{bmatrix} dS \cdot \begin{Bmatrix} u \\ \theta \end{Bmatrix} = \{F\}, \quad [9]$$

in which B_η and B_b contain the first derivatives of the finite element shape functions for respectively the element displacements u and rotations θ. The ABD matrix represents the material stiffness.

3. Results

The rubber press forming simulation was performed for an Airbus A-380 wing leading edge stiffener, manufactured by Stork Fokker AESP, as summarised in Figure 9. The pre-form of the rib was modelled using an unstructured mesh of 11055 elements. The size of the product is approximately 280 × 250 × 60 mm.

The initial fibre arrangement of the satin 8H weave glass fibre reinforced PPS laminates was a [45°/-45°|0°/90°]s, or QI, lay–up. The temperature at which the matrix material was able to sustain stresses was assumed to be 180°C. The velocity of the press was high at the beginning of the press cycle, 500 mm/s, and smoothly reduced to zero when the mould actually closed. Table 1 lists the material properties for the glass-PPS system (with a fibre volume fraction of 50%). The intraply composite data for the FRF model result from picture frame experiments at 300°C. The interply friction factor β is derived by assuming a resin rich layer of constant thickness h_{int} (0.03mm), from which

$$\beta = h_{int} / \eta \quad [10]$$

where η is the viscosity at 300°C as given by the manufacturer. Non-Newtonian behaviour is disregarded in the simulations.

The results of the draping simulation are depicted in Figure 10. Wrinkles are observed in the experiments and the simulated shape. These wrinkles are indicated with arrows and occur at the nose and next to the nose of the rib. Here, the material is actually folded. Little fibre reorientation occurred in the top surface of the product. The fabric layers only sheared approximately 5° in this area. More shearing, up to 20°, occurred in the flanges of the product.

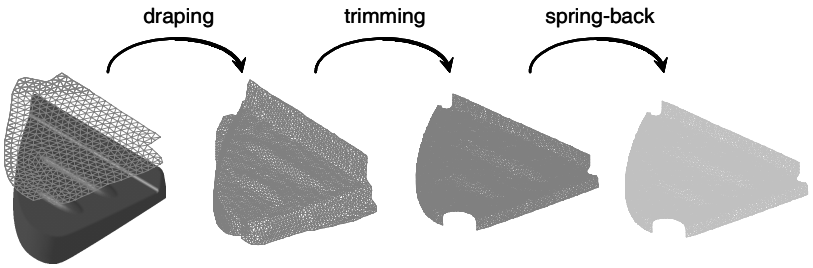

Figure 9. *RPF process simulation (from left to right): lower steel tool + laminate preform, drape result, trimming result and the deformed geometry after spring-back prediction*

Table 1. *Material properties for 8H satin glass-PPS*

fabric property			
warp count	1/m	2280	
fill count	1/m	2200	
areal density	kg/m^2	0.3	
constituent property		E-glass	PPS
Young's modulus	GPa	72.4	3.7
Poisson's ratio	-	0.23	0.37
linear thermal expansion	1/K	$5 \cdot 10^{-6}$	$51 \cdot 10^{-6}$
composite property		$\varphi \leq ½\pi$	$\varphi > ½\pi$
n	MPa	0.218	0.218
m	-	3.29	3.29
η	MPa s	0.281	0.281
η_1	Pa s	16.503	16.503
η_2	Pa s	16.503	16.503
η_3	MPa s	-0.394	0.394
η_4	MPa s	-0.394	0.394
β	m/(MPa s)	0.3	

In actual production process, the pressed rib is milled prior to mounting it in the wing leading edge. In the FE simulation, trimming was performed before the spring-back analysis, at the end of the drape simulation. The mesh reduced from 11055 elements to 7359 elements during this operation. The transition from the drape analysis into the cooling analysis was performed after trimming.

The shape distortions are predicted for two situations, either neglecting or accounting for the drape-induced fibre stresses. The out-of-plane displacements are depicted relatively to the shape of the mesh after trimming in Figure 11. The shape

distortions due to cooling are quite small when neglecting the fibre stresses. Basically, the product becomes smaller and little out-of-plane displacement, or warpage, is predicted. The absence of warpage can be explained from the fairly homogenous distribution of the fibre orientation and the accompanying coefficients of thermal expansion, even after draping. Hence, little membrane stresses are introduced.

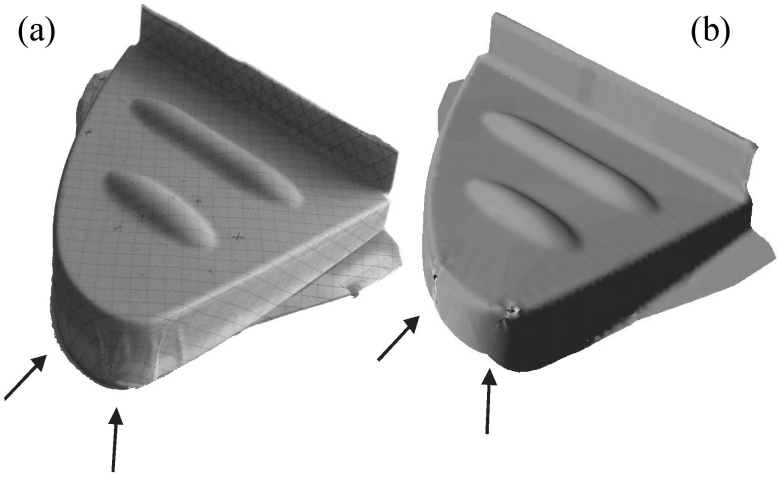

Figure 10. *Wing leading edge rib after draping: experimental (a) and simulated (b) shape. The arrows indicate the locations of wrinkles and folds*

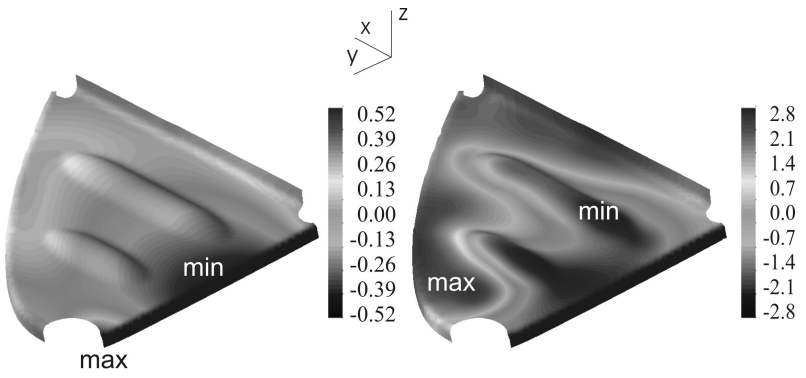

a) b)

Figure 11. *Deformed mesh of the wing leading edge rib after cooling, relative to the mesh after trimming. The contours indicate the out-of-plane displacements of the product in mm, with thermal stresses only (a) and with both thermal and fibre stresses taken into account (b)*

Significant warpage, visible as out-of-plane displacements of approximately 5 mm, is predicted when accounting for the drape-induced fibre stresses. This warpage results from the inhomogeneous distribution of the fibre stresses after draping. The inhomogeneous distribution causes membrane stresses, which in turn lead to shape distortions. The modelled CLT load and moment vector are very high and considered an overestimation of the "true" internal CLT load and moment vector. The high load vector is caused by an overestimation of the fibre stresses during the drape simulation. The maximum predicted fibre stress was approximately 1600 MPa in each of the individual layers. These stresses occurred in the area between the two cigar shaped stiffeners on the top surface of the rib.

The out-of-plane deformation of a rib was measured at Stork Fokker AESP. The rib was supported on three points, after which the coordinates of eight points on the top surface of the rib were determined with a coordinate measuring machine (Brown & Sharpe). The manufactured rib is shown in figure 12, indicating the supported and the measured points. The out-of-plane displacement is compared to the simulated results including thermal stresses only.

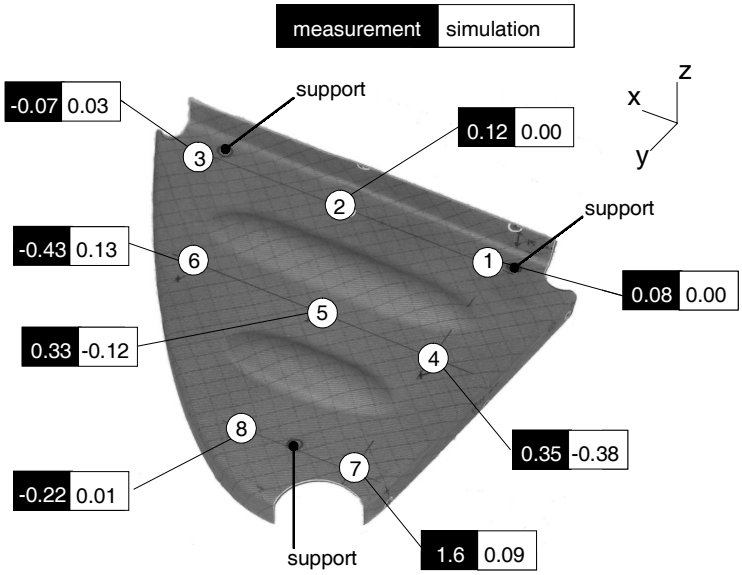

Figure 12. *Out-of-plane displacements (in mm) of eight points on the wing leading edge rib; the numbers against the black and white background denote the measured and simulated values, respectively*

The rubber pressed rib shows a large amount of skew. The right hand side warps upwards, whereas the left hand side curves downwards. Comparing points 6 and 7, the measured amount of warpage is in the order of 2 mm. The upwards displacement

near point 7 was also observed in the simulation. The rest of the global deformation pattern cannot be recognised in the simulation results.

4. Discussion

A method was presented to model the shape distortions of multi-layer woven fabric reinforced composite materials. This integral process model incorporates the fibre reorientation due to draping and the subsequent effect on the local thermo-elastic properties of the product. The fibre directions have a distinct effect on the shape distortions of the woven fabric reinforced products. A mismatch in thermal expansion in the product results in out-of-plane distortions when membrane stresses can develop. It was observed before (Lamers et al., 2002) that Quasi Isotropic lay-ups drape significantly worse than 0°/90° and 45°/-45° lay-ups. The QI lay-ups easily wrinkle and fold. Friction between the plies appears to play a dominant role in this laminate deformation process. The method presented here can be considered as a first attempt to predict the shape distortions of the composite products after forming and trimming.

The actual friction conditions, both between the plies as between the tools and the laminate, will be far more complicated than the idealised viscous description. Nesting phenomena and local fabric deformations will have an obvious effect on the laminate response under transverse interply shear conditions. Current research efforts focus on a proper characterisation of the laminate transverse shear behaviour and a suitable friction model.

The high fibre stress predictions clearly depend on the transverse interply shear stiffness. A better fabric description, incorporating the effect of fibre straightening during uniaxial and biaxial loading (Boisse et al., 2001) will also affect the fibre stress predictions. These phenomena directly affect the micro-geometry with a distinct effect on the micro-mechanics predictions of stiffnesses and residual stresses. Shear locking, as identified in (Yu et al., 2004), is also present in the elements applied here. However, the wrinkling predictions show reasonable agreement with the experiments, which supports confidence in the method presented here. The shear locking phenomenon will be investigated in more detail in the near future.

Reconsidering Figure 1, it can be observed that mainly the upper branch of the functional scheme has been presented here, to which the average laminate friction to the tool has been added. A very simple approximation of the visco-elastic behaviour of the polymer matrix has been used. Originally, the transient phenomena in cooling and crystallisation were expected to play a major role in the thermoplastic composite distortions. Model implementation and moulding experiments proved, however, that this phenomenon of through-thickness thermal gradients is not a dominant distortion mechanism for flat or shallow panels (Wijskamp et al., 2003). Instead, significant fibre stresses were identified in this particular case, due to interaction of the surface

layers with the deformable rubber tool. This surface interaction is not included in the laminate-tool friction model presented here, which only considers the average laminate deformations and displacements. Wijskamp (2005) presents further details on this type of tool interaction in our process simulations.

In addition, further tool-laminate interactions will affect the build-up of residual stresses. Stretching the laminate on a curved tool leads to resin squeeze-out, affecting the fibre content distribution through the thickness of the laminate, in turn leading to a through-thickness gradient in shrinkage and related stresses. Through-thickness temperature differences are likely to have an effect on the residual stresses, as well as the different thermal expansion of the tool and the laminate. Using two different tool materials in one process will further complicate the distortion phenomena.

The issue of high precision composite forming is clearly an area with many unsolved problems. The sum of all effects discussed here leads to a poor prediction of the measured product distortion. Important steps can be expected in the near future, however, provided an approach is chosen with a proper combination of experimental observations and numerical modelling.

5. Conclusion

A three-step method was presented to model the shape distortions of woven fabric reinforced composite materials. This integral process model incorporates the fibre reorientation due to draping and the subsequent effect on the local thermo-mechanical properties of the product. The fibre directions have a distinct effect on the shape distortions of the woven fabric reinforced products. When accounting for the drape-induced fibre stresses, significantly more shape distortions are predicted for a wing leading edge rib, with a [45°/-45°|0°/90°]s lay-up. These distortions are considered as an upper bound for the shape distortions since the drape-induced fibre stresses are considered an overestimation of the true fibre stresses. The presented approach allows for considerable improvement in the coming years, by refining various first order approximations of the composite material behaviour under forming conditions.

Acknowledgements

This work started within the EU funded PRECIMOULD project (BE97-4351) and was continued in co-operation with Ten Cate Advanced Composites and Stork Fokker Special Products, funded by the Netherlands Agency for Aerospace Programmes NIVR (BRP-49209UT). This support is gratefully acknowledged.

6. References

Avetisyan M., Meinders T., Huétink J., "Improvement of Springback Predictability after forming and trimming operations", *Esaform 2004*, p. 77-80.

Boisse P., Gasser A., Hivet G., « Analyses of fabric tensile behaviour: determination of the biaxial tension–strain surface and their use in forming simulations », *Composites: Part A*, Vol. 32, 2001, p. 1395-1414.

Hashin Z., "Analysis of Composite Materials – A Survey", *Journal of Applied Mechanics*, Vol. 50, 1983, p. 481-505.

Hofstee J., De Boer H., Van Keulen F., "Elastic stiffness analysis of thermo-formed plain-weave composite part III: experimental verification", *Composites Science & Technology* Vol. 62, 2002, p. 401-418.

Hsiao S.-W., Kikuchi N., "Numerical analysis and optimal design of composite thermoforming process", *Computer Methods in Applied Mechanics and Engineering*, Vol. 177, 1999, p. 1-34.

Lamers E.A.D, Wijskamp S., Akkerman R., "Modelling the thermo-elastic properties of skewed woven fabric reinforced composites", *ECCM 9*, 2000, CD proceedings.

Lamers E.A.D, Akkerman R., Wijskamp S., "Fibre Orientation Modelling for Rubber Press Forming of Thermoplastic Laminates", *International Journal of Forming Processes*, 2002, p. 443-463.

Lamers E.A.D, Wijskamp S., Akkerman R., "Drape Modelling of Multi-Layered Composites", *Esaform 2003*, p. 323-326.

Lamers E.A.D., Akkerman R., Wijskamp S., "*Multilayer Drape Modelling of Thermoplastic Laminates",* submitted to *Composites: Part A*, 2004.

Lamers E.A.D, Shape Distortions in Fabric Reinforced Composite Products Due to Processing Induced Fibre Reorientation, PhD Thesis University of Twente, 2004.

Meinders T., Van den Boogaard A. H., Huétink J., "Improvement of implicit finite element code performance in deep drawing simulations by dynamics contributions", *Journal of Materials Processing Technology*, Vol. 134, 2003, p. 413-420.

Schapery R., "Thermal expansion coefficients of composite materials based on energy principles", *Journal of Composite Materials*, Vol. 2, 1968, p. 380-404.

Spencer A.J.M., "Theory of fabric-reinforced viscous fluids", *Composites: Part A*, Vol. 31, 2000, p. 1311-1321.

Sweeting R., Liu X., Paton R., "Prediction of processing-induced distortion of curved flanged composite laminates", *Composite Structures*, Vol. 57, 2002, p. 79-84.

Van Haaren M.J., Stoker H.C., Van den Boogaard A.H., Huétink J., "The ALE-method with triangular elements: direct convection of integration point values", *International Journal for Numerical Methods in Engineering*, Vol. 49, 2000, p. 697-720.

Vreede P.T., A finite element method for simulations of 3-dimensional sheet metal forming, PhD Thesis University of Twente, 1992.

Wiersma H.W., Peeters L.J.B., Akkerman R., "Prediction of springforward in continuous-fibre/polymer L-shaped parts", *Composites Part A*, Vol. 29A, 1998, p. 1333-1342.

Wijskamp S., Lamers E.A.D., Akkerman R., "Residual stresses in rubber formed thermoplastic composites", *Esaform 2003*, p. 855-858.

Wijskamp S., Shape Distortions in Composites Forming, PhD thesis University of Twente, 2005.

Yu X., Ye L., Mai Y.-W., "Finite Element Spurious Wrinkles on the Thermoforming Simulation of Woven Fabric Reinforced Composites", *Esaform 2004*, p. 325-328.